

RESEARCH PAPER

Synthesis and Characterization of CuO/CeO₂ Nanocomposites and Investigation Their Photocatalytic Activity

Ban Hasan Taresh¹, Faten Hadi Fakhri² and Luma M. Ahmed^{2*}

¹ Department of Clinical Laboratories, College of Applied Medical Sciences, University of Kerbala, Kerbala, Iraq

² Department of Chemistry, College of Science, University of Kerbala, Kerbala 56001, Iraq

ARTICLE INFO

Article History:

Received 29 April 2022

Accepted 21 June 2022

Published 01 July 2022

Keywords:

CuO/CeO₂

Hydrothermal

Photocatalysis

Nanocomposite

Organic pollutant

ABSTRACT

In this work, CuO/CeO₂ nanocomposite was prepared via hydrothermal route. The product was prepared under 12 h and 150 °C. The shape, size, and crystalline structure have been investigated through using various techniques such as the scanning electron microscopy (SEM), with energy dispersive X-ray (EDX), the X-ray diffraction analysis (XRD), the Fourier transform infrared spectroscopy (FTIR), and thermogravimetric analysis (TGA). The magnetic properties of prepared nanocomposites were studied via vibrating-sample magnetometer (VSM). Consequently, acid violet and rhodamine B dyes were applied for investigation the photocatalytic activity of prepared CuO/CeO₂ nanocomposite. Results showed that Acid violet and rhodamine B were photo-decolorization under UV irradiation after 120 minutes with 95.8 % and 88.2% respectively. This excellent performance was due to the suitable band structure of synthesized CuO/CeO₂ nanocomposites which led to depress the recombination of photo-generated electrons and holes with increased the acidity of CeO₂ after incorporation it with CuO in the crystal lattice. This work introduces new nanocomposites for decolorization of organic pollutants from wastewater.

How to cite this article

Taresh B H., Fakhri FH., Ahmed L M. Synthesis and Characterization of CuO/CeO₂ Nanocomposites and Investigation Their Photocatalytic Activity. J Nanostruct, 2022; 12(3):563-570. DOI: 10.22052/JNS.2022.03.009

INTRODUCTION

The development of numerous unique functional and smart materials is dependent on the development of a particular class of nanomaterials [1-3]. Because of their unique physical and chemical properties, the transition metal oxide (TMO)-based nanomaterials have been attracting a lot of attention [4-6]. Till now, these nanostructures have been applied for a variety of industrial applications. High specific surface area, higher surface energy and quantum confinement are responsible for the attractive physical and chemical properties in TMO

* Corresponding Author Email: luma.ahmed@uokerbala.edu.iq

nanomaterials [7-9]. Since these features are vast pauper on the size and shape of nanoparticles, it is essential to apply a suitable method for preparation TMO nanostructures with desired shape and morphology [10-12]. So, various metal oxide nanostructures with different properties have been prepared and applied in various fields [13-16].

Because of its intriguing features as a p-type semiconductor with a narrow band gap and as the basis of various high-temperature superconductors, cupric oxide (CuO) has been found more attention in TMO research [17-



This work is licensed under the Creative Commons Attribution 4.0 International License.

To view a copy of this license, visit <http://creativecommons.org/licenses/by/4.0/>.

19]. CuO nanomaterials with high surface-to-volume ratio, and potential size effects have excellent chemical and physical features that are vastly different from those of their micro or bulk counterparts [20, 21]. The promising applications of these nanostructures have been thoroughly explored. CuO nanomaterials have attractive structural properties that make them an ideal platform for the composite construction with various components to improve its different photocatalytic and bio-related application. So, the binary design of CuO nanomaterials mixed with inorganic nanostructures is the most popular choice used for preparation of effective nanocomposites [22, 23]. Cerium dioxide, CeO₂ has received a lot of interest in recent years due to its widespread availability and high potential of catalyst-based application. CeO₂ has a large oxygen storage capacity, abundant oxygen vacancies, and the ability to flip between Ce³⁺ and Ce⁴⁺ with ease [24-26].

Jianyu Yun et al. prepared CuO/CeO₂ nanocomposites using the non-equilibrium plasma, and then comparing with the traditional calcination. Results revealed that the treatment of non-equilibrium plasma after calcination

can considerably improve the synergism effect between the CuO active phase and the CeO₂ support, which leading to good dispersion of CuO. They applied CuO/CeO₂ nanocomposites as an effective catalyst for toluene oxidation [27].

Weiwei Jie et al. prepared the 1D cerium oxide nanotubes, nanowires, and nanorods via hydrothermal route and supported CuO for CO preferential oxidation. They characterized the products via XRD and TEM analysis. It is found that CuO/CeO₂ nanotubes had the highest CO oxidation activity [28].

In this work, the CuO/CeO₂ nanocomposite was synthesized via simple and novel hydrothermal route. The prepared sample was characterized to prove synthesis it via using different techniques such as XRD, SEM, EDX, FTIR, and TGA. The results showed that prepared CuO/CeO₂ nanocomposites can be applied in different applications.

MATERIALS AND METHODS

Chemicals and instruments

All chemicals were of synthesis grade, obtained from Scharlau, and used without extra purification. Nanoscale composites were characterized by Philips-X' pertpro X-ray diffraction analysis that

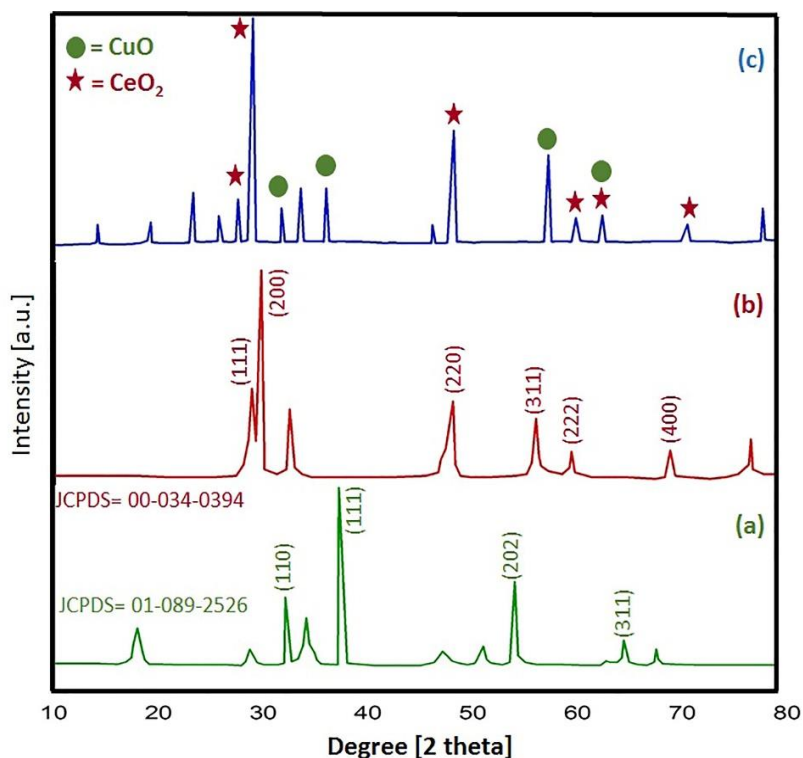


Fig. 1. The XRD pattern of a) pure CuO, b) pure CeO₂, and c) CuO/CeO₂ NCs.

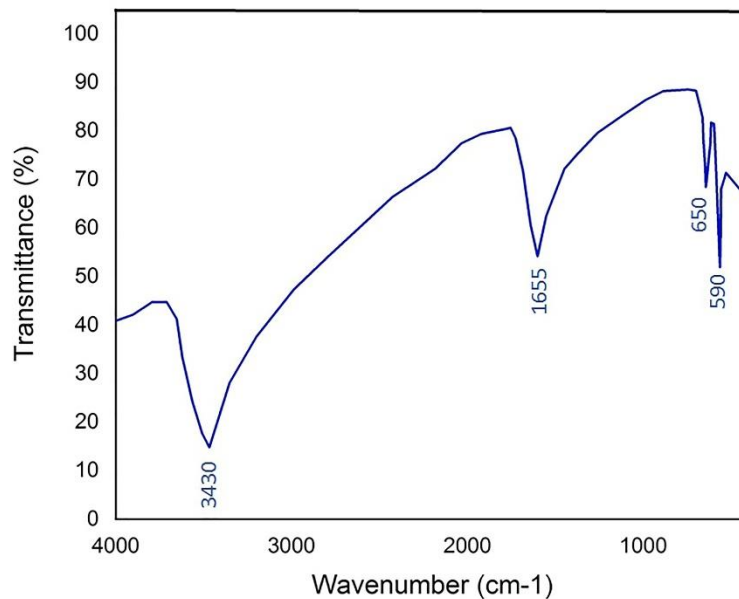


Fig. 2. FT-IR spectrum of CuO/CeO₂ NCs.

employing Ni-filtered Cu K α radiation. Also, the FT-IR spectra was carried out for solid sample using KBr pellets, Nicolet Magna 550 FT-IR spectrometer. The morphological engineering and particle size for prepared sample were detected using LEO-1455VP Field-Emission scanning electron microscopy with an energy dispersive X ray spectroscopy.

Preparation of CuO nanoparticles (CuO NPs)

0.5 g CuSO₄·2H₂O was added to 50 mL DI water under stirrer conditions. After, as-prepared sodium hydroxide solution (10 M) were added. The obtained mixture was moved to a Teflon-lined stainless steel autoclave and heated at 150 °C for 10 h. The final product was filtered, washed with ethanol, and dried at 65 °C.

Preparation of CeO₂ nanoparticles (CeO₂ NPs)

Firstly, 0.6 g Ce(SO₄)₂·4H₂O in 50 mL DI water were completely dissolved at 50 °C. Next, sodium hydroxide solution (10 M) were added into above solution. After that, the mixture was put into a Teflon-lined stainless steel autoclave and heated at 150 °C for 12 h. the resultant powder was filtered, washed with ethanol, and dried at 65 °C.

Preparation of CuO/CeO₂ nanocomposites (CuO/CeO₂ NCs)

The nanoscale CuO/CeO₂ composites was

prepared as following: Initially, CuSO₄·2H₂O and Ce(SO₄)₂·4H₂O were dissolved completely in DI water (25 mL) at room temperature. Under continuous stirring, the as-prepared sodium hydroxide solution (10 M) was added drop by drop to above solution. After that, the mixture was stirred at 25 °C for 10 min. Then, the mixture was transferred to a Teflon-lined stainless steel autoclave and kept under hydrothermal conditions (150 °C, 12 h). After the completion of the reaction time, the dark solid was brought to ambient temperature, filtered, washed with ethanol, and dried at 65 °C. The product was finally calcined at 600 °C for 2 h.

RESULT AND DISCUSSION

The identification of composition structure was confirmed by XRD technique. Fig. 1a shows the XRD graph of the pure CuO NPs. The position and intensity ratio of these peaks have acceptable to reference pattern (JCPDS= 01-089-2529) [29]. Besides, CuO NPs Miller's index is seen. According to the Debye-Scherrer equation ($D = k\lambda / \beta \cos\theta$) [30-32], the crystallite size was calculated approximately 48 nm. Today, many papers have been published about XRD patterns of the CeO₂ NPs. The obtained XRD patterns of CeO₂ NPs (JCPDS= 00-034-0394) in this study is totally in agreement with previous report [33]. The number

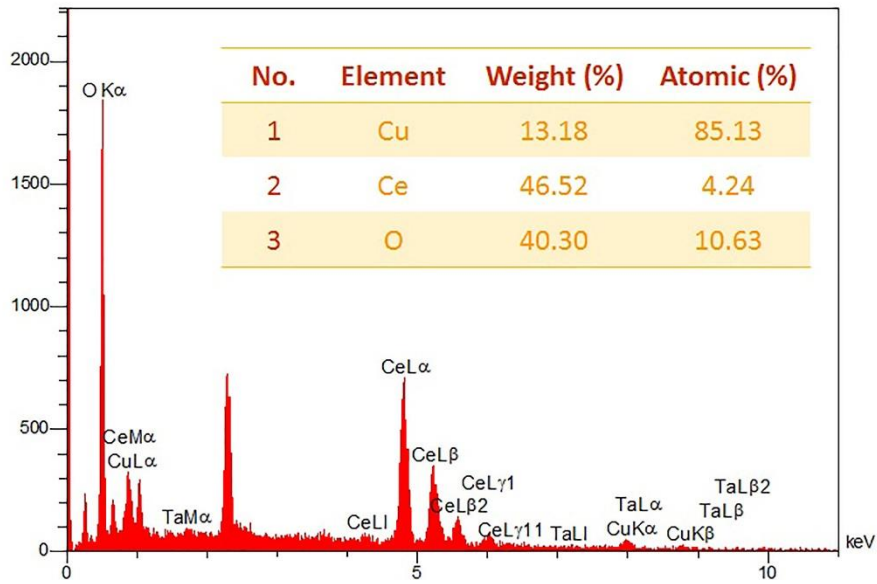


Fig. 3. EDX analysis of CuO/CeO₂ NCs.

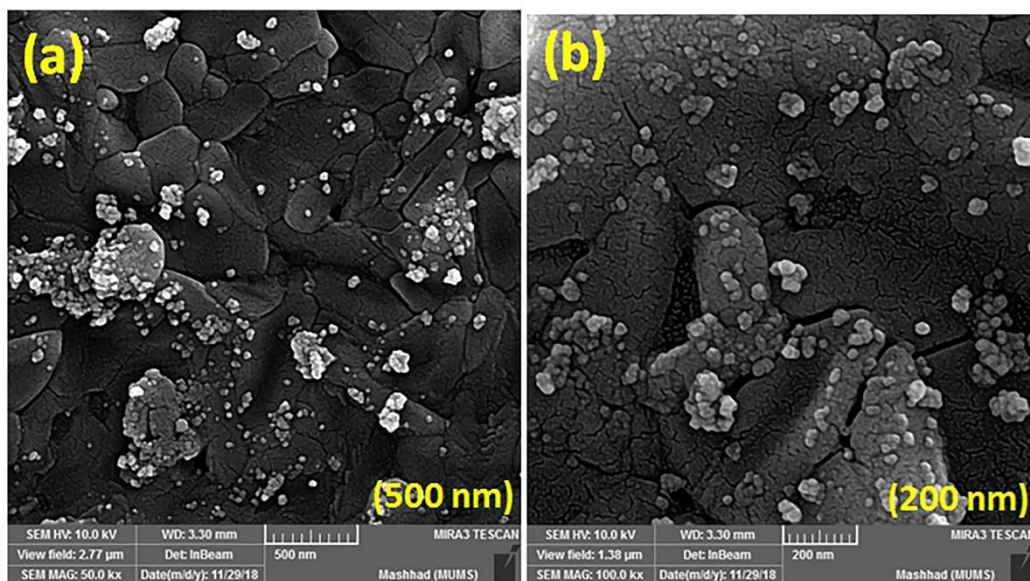


Fig. 4. FE-SEM images of CuO/CeO₂ NCs.

of clear diffraction and peaks of CeO₂ NPs are observed in Fig. 1b. The CeO₂ crystallite size, which is measured by the Debye equation, was reported 38 nm. Almost all Miller peaks of pure CuO and CeO₂ NPs are displayed in final XRD patterns and the 2θ of CeO₂ elevate when CuO incorporated with the crystal lattice of CeO₂ by metal-metal bond that same results which reported in reports

[34,35] (Fig. 1c). Accordingly, the CuO/CeO₂ NCs have been successfully fabricated as nanocomposite with the crystallite size about 56 nm.

The surface functional group was studied by FT-IR test. Fig. 2 shows the FT-IR spectrum of CuO/CeO₂ NCs synthesized by hydrothermal route. As showed peaks in 3430 cm⁻¹ and 1655 cm⁻¹ are related to hydroxyl group stretching and bending

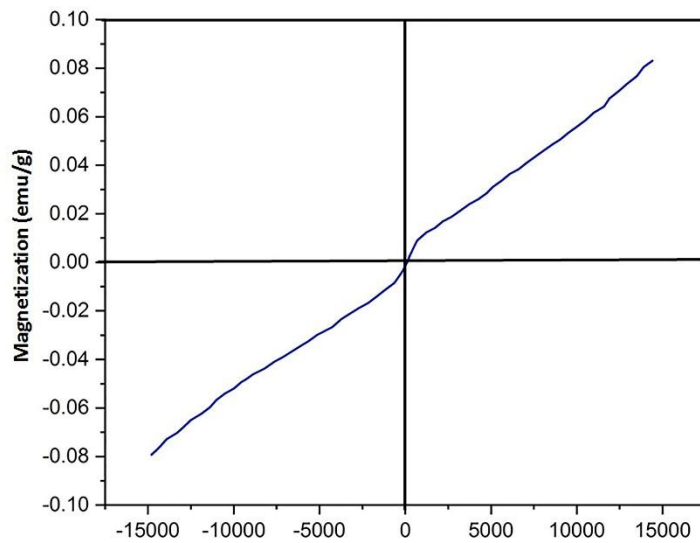


Fig. 5. VSM analysis of CuO/CeO₂ NCs.

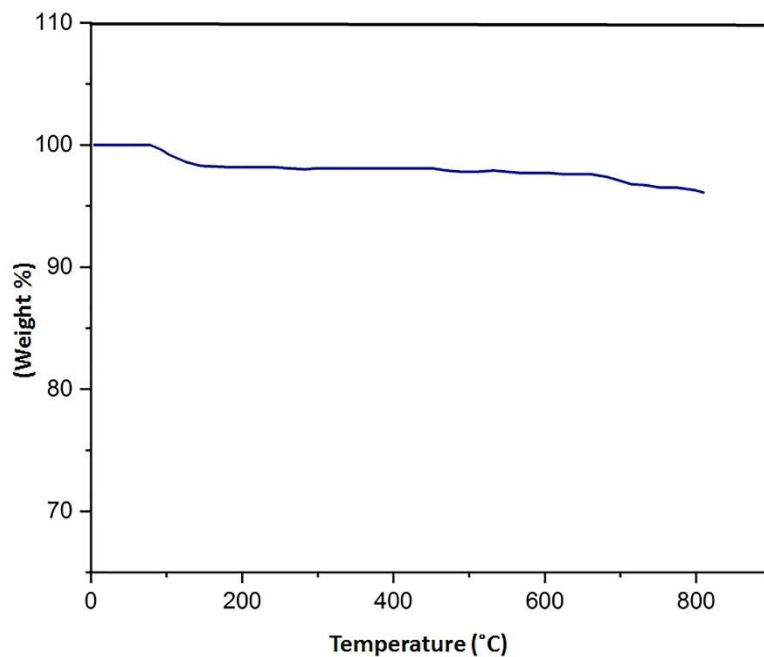


Fig. 6. TGA curve of CuO/CeO₂ NCs.

absorption of water, respectively, which similar the position of water OH in metal oxides[36,37]. Also, the peaks at 650 cm⁻¹ and 590 cm⁻¹ correspond to Ce-O and Cu-O, respectively that attitude to the reduced mass for Cu-O is less than value for Ce-O, and the wave number is more for Ce-O.

The purity of CuO/CeO₂ NCs was confirmed by EDX analysis in Fig. 3. In this analysis, cerium,

copper, and oxygen are the main elements. This test could be concluded that the CuO/CeO₂ NCs are formed without any impurity, and the summation of atoms equal to 100%.

The morphological property of CuO/CeO₂ NCs was found by using FE-SEM spectroscopy (Fig. 4). Based on FE-SEM images, it can be understood that CuO and CeO₂ nanoparticles have been gone

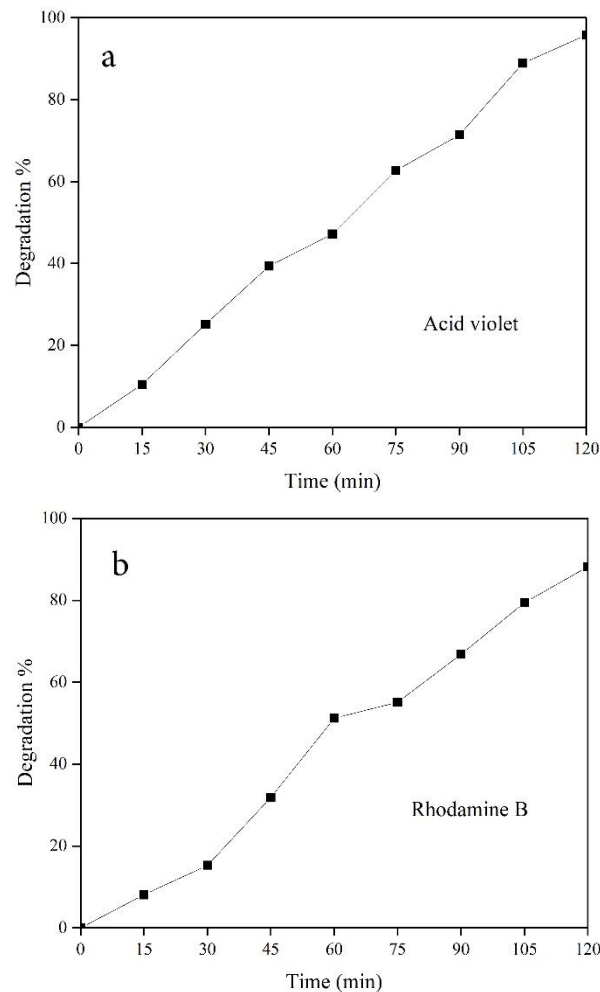


Fig. 7: Photocatalytic activity of CuO/CeO₂ nanocomposites against a) Acid violet 7 b) Rhodamine B.

together as a semi-spherical plate.

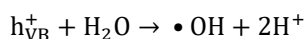
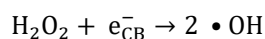
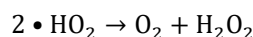
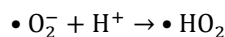
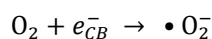
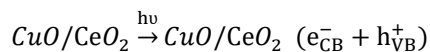
Also, the magnetization attributes of CuO/CeO₂ NCs was determined with the help of a VSM analysis (Fig. 5). Data display that the magnetization amount was reported about 0.08 emu/g.

Based on Fig. 6, the thermogravimetric analysis was applied to find the thermal stability of the CuO/CeO₂ NCs. This nanocomposite reveals a suitable thermal stability without a significant decline in CuO/CeO₂ NCs weight. The weight loss about (2%) at temperatures below 180 °C is owing to the removal of physically adsorbed solvent and surface hydroxyl groups. Rising temperature up to 800 °C is related to decompose of nanocomposites structure.

The photocatalytic activity of prepared CuO/CeO₂ nanocomposites was studied toward acid violet 7 and rhodamine B under UV irradiation using % Efficiency = $\frac{[(1-C_{dye,t}) / (1-C_{dye,0})] \times 100}{C_{dye,0}}$ when C_{dye,0} is the initial concentration of dye at t zero (dark reaction), and at t time of reaction C_{dye,t} is a concentration of the same studied dye [37-40] at wavelengths 517 nm and 510 nm for acid violet 7 and rhodamine B, respectively.

The Fig. 7 shows % of photo-degradation efficiency of acid violet 7 and rhodamine B after 120 min. As well as shown, the 95.8 % and 88.2% of acid violet 7 and rhodamine B was photodecolorization after 120 min irradiation. This excellent function can be attributed to the synergism between CuO and CeO₂ nanostructures.

The possible mechanism can be provided for photodegradation of any dyes [41-44] such as (acid violet 7 and rhodamine B) in presence of photocatalyst:



Degradation of Acide violet 7 (Rhodamine B)

CONCLUSION

In conclusion, the CuO/CeO₂ nanocomposite was synthesized via in-situ hydrothermal route. The prepared products were characterized via XRD, SEM, FTIR, VSM, VSM and TGA analysis. The characterization techniques confirmed the formation of the CuO/CeO₂ nanocomposites with any impurity. Morphological investigation revealed semi-spherical plate morphology of CuO and CeO₂ in linking together. The prepared semiconductor nanocomposites were applied for photodegradation of acid violet and rhodamine B under ultraviolet irradiation. The results showed the excellent photocatalytic performance of prepared CuO/CeO₂ nanocomposites that beyond to improve the surface properties for CuO and CeO₂ such as increased the acidity of surface, depressed the recombination after formed their nanocomposite. It was found that 95.8 and 88.2% of acid violet 7 and rhodamine B was removed through treatment via CuO/CeO₂ nanocomposites. The provided mechanism showed that the free hydroxyl radicals are the responsible for photocatalytic activity of CuO/CeO₂ nanocomposites.

CONFLICT OF INTEREST

The authors declare that there is no conflict

of interests regarding the publication of this manuscript.

REFERENCES

- Roduner E. Size matters: why nanomaterials are different. *Chem Soc Rev.* 2006;35(7):583-592.
- Chen G, Seo J, Yang C, Prasad PN. Nanochemistry and nanomaterials for photovoltaics. *Chem Soc Rev.* 2013;42(21):8304-8338.
- Bréchnignac C, Houdy P, Lahmani M. *Nanomaterials and nanochemistry: Springer Science & Business Media; 2008.*
- Jia Y, Yi X, Li Z, Zhang L, Yu B, Zhang J, et al. Recent advance in biosensing applications based on two-dimensional transition metal oxide nanomaterials. *Talanta.* 2020;219:121308.
- Kastl AM, Purdy AP, Butcher RJ. Synthesis of early transition metal oxide nanomaterials and their conversion to nitrides. *Journal of Nanoparticle Research.* 2020;22(10):1-15.
- Maduraiveeran G. Nanoporous structured mixed transition metal oxides nanomaterials for electrochemical energy conversion technologies. *Materials Letters.* 2021;283:128763.
- Veerakumar P, Sangili A, Manavalan S, Thanasekaran P, Lin K-C. Research progress on porous carbon supported metal/ metal oxide nanomaterials for supercapacitor electrode applications. *Ind Eng Chem Res.* 2020;59(14):6347-6374.
- Saleem M, Tiwari S, Soni M, Bajpai N, Mishra A. Structural, optical and other spectral studies of transition metal Ti 4+-doped Zn-Cd oxide nanomaterials. *International Journal of Modern Physics B.* 2020;34(06):2050033.
- Ganachari SV, Hublikar L, Yaradoddi JS, Math SS. Metal oxide nanomaterials for environmental applications. *Handbook of Ecomaterials.* 2019;4:2357-2368.
- Kronawitter CX, Bakke JR, Wheeler DA, Wang W-C, Chang C, Antoun BR, et al. Electron enrichment in 3d transition metal oxide hetero-nanostructures. *Nano Lett.* 2011;11(9):3855-3861.
- Hang MN, Hudson-Smith NV, Clement PL, Zhang Y, Wang C, Haynes CL, et al. Influence of nanoparticle morphology on ion release and biological impact of nickel manganese cobalt oxide (NMC) complex oxide nanomaterials. *ACS Applied Nano Materials.* 2018;1(4):1721-1730.
- Heard CJ, Čejka J, Opanasenko M, Nachtigall P, Centi G, Perathoner S. 2D oxide nanomaterials to address the energy transition and catalysis. *Advanced Materials.* 2019;31(3):1801712.
- Mei J, Liao T, Kou L, Sun Z. Two-dimensional metal oxide nanomaterials for next-generation rechargeable batteries. *Advanced Materials.* 2017;29(48):1700176.
- Kumar RR, Kumar KU, Haranath D. *Synthesis, Properties, and Applications of Transition Metal Oxide Nanomaterials. Multifunctional Nanostructured Metal Oxides for Energy Harvesting and Storage Devices: CRC Press; 2020. p. 1-73.*
- Abdah MAAM, Azman NHN, Kulandaivalu S, Sulaiman Y. Review of the use of transition-metal-oxide and conducting polymer-based fibres for high-performance supercapacitors. *Materials & Design.* 2020;186:108199.
- Xing Y, Cai Y, Cheng J, Xu X. Applications of molybdenum oxide nanomaterials in the synergistic diagnosis and treatment of tumor. *Applied Nanoscience.* 2020;10(7):2069-2083.
- Chen Y, Zhang L, Zhang H, Zhong K, Zhao G, Chen G, et al. Band gap manipulation and physical properties of preferred

- orientation CuO thin films with nano wheatear array. *Ceramics International*. 2018;44(1):1134-1141.
18. Abdullah OG, Aziz SB, Omer KM, Salih YM. Reducing the optical band gap of polyvinyl alcohol (PVA) based nanocomposite. *Journal of Materials Science: Materials in Electronics*. 2015;26(7):5303-5309.
 19. ur Rehman A, Aadil M, Zulfiqar S, Agboola PO, Shakir I, Aboud MFA, et al. Fabrication of binary metal doped CuO nanocatalyst and their application for the industrial effluents treatment. *Ceramics International*. 2021;47(5):5929-5937.
 20. Wang W, Zhou Q, Fei X, He Y, Zhang P, Zhang G, et al. Synthesis of CuO nano-and micro-structures and their Raman spectroscopic studies. *CrystEngComm*. 2010;12(7):2232-2237.
 21. Subalakshmi P, Sivashanmugam A. CuO nano hexagons, an efficient energy storage material for Li-ion battery application. *Journal of Alloys and Compounds*. 2017;690:523-531.
 22. Chang T, Li Z, Yun G, Jia Y, Yang H. Enhanced photocatalytic activity of ZnO/CuO nanocomposites synthesized by hydrothermal method. *Nano-Micro Letters*. 2013;5(3):163-168.
 23. Shanmugavani A, Selvan RK. Improved electrochemical performances of CuCo₂O₄/CuO nanocomposites for asymmetric supercapacitors. *Electrochimica Acta*. 2016;188:852-862.
 24. Raees A, Jamal MA, Ahmed I, Silanpaa M, Saad Algarni T. Synthesis and characterization of CeO₂/CuO nanocomposites for photocatalytic degradation of methylene blue in visible light. *Coatings*. 2021;11(3):305.
 25. Cam TS, Vishnievskaja TA, Popkov VI. Catalytic oxidation of CO over CuO/CeO₂ nanocomposites synthesized via solution combustion method: effect of fuels. *Reviews on Advanced Materials Science*. 2020;59(1):131-143.
 26. Mousavi-Kamazani M, Rahmatolahzadeh R, Beshkar F. Facile solvothermal synthesis of CeO₂-CuO nanocomposite photocatalyst using novel precursors with enhanced photocatalytic performance in dye degradation. *Journal of Inorganic and Organometallic Polymers and Materials*. 2017;27(5):1342-1350.
 27. Yun J, Wu L, Hao Q, Teng Z, Gao X, Dou B, et al. Non-equilibrium plasma enhanced oxygen vacancies of CuO/CeO₂ nanorod catalysts for toluene oxidation. *Journal of Environmental Chemical Engineering*. 2022:107847.
 28. Jie W, Liu Y, Deng W, Liu Q, Qiu M, Liu S, et al. Effect of one-dimensional ceria morphology on CuO/CeO₂ catalysts for CO preferential oxidation. *J Solid State Chem*. 2022;311:123109.
 29. Berra D, Laouini S, Benhaoua B, Ouahrani M, Berrani D, Rahal A. Green synthesis of copper oxide nanoparticles by Pheonix dactylifera L leaves extract. *Digest Journal of Nanomaterials and Biostructures*. 2018;13(4):1231-1238.
 30. Ali S, Ali M, Ahmed L. Hybrid Phosphotungstic acid-Dopamine (PTA-DA) Like-flower Nanostructure Synthesis as a Furosemide Drug Delivery System and Kinetic Study of Drug Releasing. *Egyptian Journal of Chemistry*. 2021;64(10):5547-5553.
 31. Jassim S, Abbas A, AL-Shakban M, Ahmed L. Chemical Vapour Deposition of CdS Thin Films at Low Temperatures from Cadmium Ethyl Xanthate. *Egyptian Journal of Chemistry*. 2021;64(5):2533-2538.
 32. Alkhafaji EN, Oda NA, Ahmed LM. Characterization of silver nanohybrid with layers double hydroxide and demonstration inhibition of antibiotic-resistance Staphylococcus aureus. *Egyptian Journal of Chemistry*. 2022;65(6):1-2.
 33. Zarezadeh Mehrizi M, Ahmadi S, Beygi R, Asadi M. Fabrication of cerium oxide nanoparticles by solution combustion synthesis and their cytotoxicity evaluation. *Russian Journal of Non-Ferrous Metals*. 2018;59(1):111-116.
 34. Obaid AJ, Ahmed L. One-step hydrothermal synthesis of α-MoO₃ nano-belts with ultrasonic assist for incorporating TiO₂ as a nanocomposite. *Egyptian Journal of Chemistry*. 2021;64(10):3-4.
 35. Kadhim H, Ahmed L, AL-Hachamii M. Facile Synthesis of Spinel CoCr₂O₄ and Its Nanocomposite with ZrO₂: Employing in Photo-catalytic Decolorization of Fe (II)-(luminol-Tyrosine) Complex. *Egyptian Journal of Chemistry*. 2022;65(1):481-488.
 36. Ahmed LM, Ivanova I, Hussein FH, Bahnemann DW. Role of platinum deposited on TiO₂ in photocatalytic methanol oxidation and dehydrogenation reactions. *International Journal of Photoenergy*. 2014;2014.
 37. Ahmed LM, Hussein FH, Mahdi AA. Photocatalytic dehydrogenation of aqueous methanol solution by naked and platinized TiO₂ nanoparticles. *Asian J Chem*. 2012;24(12):5564.
 38. Fakhri FH, Ahmed LM. Incorporation CdS with ZnS as composite and using in photo-decolorization of congo red dye. *Indonesian Journal of Chemistry*. 2019;19(4):936-943.
 39. Jawad TM, R AL-Lami M, Hasan AS, Al-Hilifi JA, Mohammad RK, Ahmed L. Synergistic Effect of dark and photoreactions on the removal and photo-decolorization of azo carmosine dye (E122) as food dye using Rutile-TiO₂ suspension. *Egyptian Journal of Chemistry*. 2021;64(9):4857-4865.
 40. Ridha NJ, Alosfur FKM, Kadhim HBA, Ahmed LM. Synthesis of Ag decorated TiO₂ nanoneedles for photocatalytic degradation of methylene blue dye. *Materials Research Express*. 2021;8(12):125013.
 41. Hussain ZA, Fakhri FH, Alesary HF, Ahmed LM, editors. ZnO Based Material as Photocatalyst for Treating the Textile Anthraquinone Derivative Dye (Dispersive Blue 26 Dye): Removal and Photocatalytic Treatment. *Journal of Physics: Conference Series*; 2020: IOP Publishing.
 42. Hussein ZA, Abbas SK, Ahmed LM, editors. UV-A activated ZrO₂ via photodecolorization of methyl green dye. *IOP Conference Series: Materials Science and Engineering*; 2018: IOP Publishing.
 43. Kzar KO, Mohammed ZF, Saeed SI, Ahmed LM, Kareem DI, Hadyi H, et al., editors. Heterogeneous photo-decolourization of cobaltous phthalocyanine dye (Reactive green dye) catalyzed by ZnO. *AIP Conf Proc*; 2019: AIP Publishing LLC.
 44. Ahmed LM, Saeed SI, Marhoon AA. Effect of oxidation agents on photo-decolorization of vitamin B 12 in the presence of ZnO/UV-A system. *Indonesian Journal of Chemistry*. 2018;18(2):272-278.